In silico Evaluation of Selected Phytochemicals for Anti-nCovid Potential Based on Molecular Docking Studies and Their Pharmacokinetics and Drug-likeness Predictions

Venkatachalam Thangavel[1]Selvapraba S[1], Senthil Kumar N[1], Kalaiselvi P[1], Saravannan D[2]

[1]*JKKMMRF's – Annai JKK Sampoorani Ammal College of Pharmacy, Komarapalayam, Namakkal – 638 183*.The Tamil nadu Dr MGR Medical University,Chennai,600032

[2]Tagore College of Pharmacy, Vandalur-Kelampakkam Road, Rathinamangalam,Chennai, Tamil Nadu-600127.

ABSTRACT

SARS-CoV-2 has devastated the world with its rapid spread and fatality. Pharmaceutical giants respective of their market has stretched towards research and enhancing the productive capacities of their units to meet the unprecedented drug demand. Drug discovery approaches involving all in silico, in vitro, in vivo approaches to design and develop has fastened. The present work explains in-silico drug discovery methods like molecular docking and molecular dynamic simulations to screen for highly probable, safe, and effective phytochemical principles against SARS-CoV-2. Docking of various phytochemical principles against three X-ray crystallographic and one electron microscopic structures of SARS-CoV-2 proteins that include the RNA dependent RNA polymerase and 3CL protease (3CL pro) by using the Glide Schrodinger docking software 2019_4. 3.1 was carried out. The best fit drug candidates among the docked ligand structures by their docking score and interactions were selected and subjected to prediction of drug likeliness and ADME parameters. It is observed that the phytochemicals/bioactives such as Scutellarein, Saikosaponin D, Syringaresinol and 5,7,2',3-Tetramethoxyflavone hold promise in inhibiting the SARS-CoV-2 key viral proteins and displayed the capability to suppress SARS-CoV-2 proteins and justify their further in vitro and in vivo studies. The present study could be the starting point for the future ligands from natural sources in 2019-nCoV RdRp and 3CL pro.

Corresponding author
Dr Venkatachalam Thangavel
Professor & Head
Department of pharmaceutical chemistry,
JKKMMRF's-Annai JKK Sampoorani ammal college of Pharmacy,
Ethirmedu,Vattamalai,B.Komarapalayam,Namakkal DT,
Tamilnadu-638183

1.Introduction

The mankind was terribly wobbled, troubled and lead to catastrophy in every domain by the most infectious and deadly COVID -19 virus. The entire world has to face a crisis that it may wipe out the human kind. Almost every nuke and corner has thoroughly put under intense pressure to carry out research and validate the findings to contain the infection, be it may be developing sanitizers, PPEs, diagnostic kits, biomedical equipment, and most importantly to design novel agents as well testing the existing ones for repurpose to treat this novel virus. In the coronaviridae family of viruses 2019-nCoV is a novel strain not identified earlier in humans (Ji Wet al., 2020)[1]. The initial outburst of 2019-nCoV in the epicenter of Wuhan province in China has spread briskly and affected other parts of China. Soon or a little later the entire world was afflicted and faced enormous challenge and health care burden(Wu JT et al., 2020)[2]. The lethality of 2019-nCoV epidemic is unprecedently larger than the severe acute respiratory syndrome (SARS) epidemic. World Health Organization (WHO) has declared nCoV as pandemic on 11 March 2020, and gave the nomenclature as nCovid-19 COVID-19 and declared as 'Public Health Emergency of International Concern' (PHEIC), affecting around 212 countries and accounting for nearly 1 million deaths across the globe. In this scenario, WHO has issued the COVID-19 advisory from time to time through WHO website (WHO, 2020)[3]. Pharmaceutical giants respective of their market has stretched towards research and enhancing the productive capacities of their units to meet the unprecedented drug demand. Biotech firms and Vaccine manufacturers all over the globe are thoroughly designing and evaluating the vaccines which are a time taking and under stringent regulatory standards. Drug discovery approaches involving all in silico, in vitro, in vivo approaches to design and develop has fastened. In silico paradigms have much larger role in enhancing high throughput screening efforts. Particularly, in-silico studies have great role of finding magic molecules and repurposing of existing drugs in the treatment of COVID-19 (Beura S et al., 2020)[4]. Earlier in 2003 SARS epidemic, the effectiveness of herbal treatments was demonstrated and gained huge prominence. Hence as demanded by the need and thrust, to find the therapeutics to lessen the COVID induced mortality. Complementary and alternative medicine systems were largely focused their research to evolve prospective molecules.

The single-stranded RNA genome of SARS-COV-2 is depicted in Figure 1.

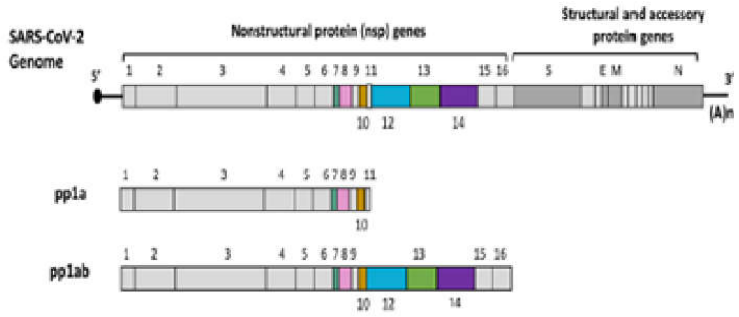

Figure 1: Single-Stranded RNA Genome of SARS-CoV-2

Two-thirds of the genome encodes two large polyproteins, pp1a and pp1ab, that are cleaved into 16 non-structural proteins. The last one-third of the genome encodes structural and accessory proteins. This figure was created with BioRender.

The studies on SARS-CoV-2 as well as previous SARS-CoV and other coronaviruses have mostly identified with the functions of these structural proteins, non-structural proteins as well as accessory proteins.Thus, keeping the above view into consideration, the present investigation was undertaken to determine the efficacy of 48 different phytoconstituents in comparison to reference drugs (Remdesivir) against two different protein targets, that is, RNA dependent RNA polymerase and 3CL pro using in-silico docking.

2. Materials and methods

2.1.1 Computational studies

The molecular docking studies and molecular dynamics analysis were performed using Glide Schrodinger docking software 2019_4. 3.1.

2.1.2 SARS-COV-2 drug targets

The following SARS-COV-2 proteins were obtained from the RSCB-Protein Data Bank using PDB codes that include: (i) the RNA dependent RNA polymerase (PDB ID: 6M71), (ii) 3CL protease (3CL pro) (PDB ID: 6M2N)

Targeting RNA-dependent RNA polymerase (6M71)

6M71 is an unligandedelectron cryo-microscopic structure of SARS-CoV-2 RNA-dependent RNA polymerase in complex with cofactors and other likely assembles at 2.90 Å. The structure consists of four polypeptide chains (A, B, C, D); RNA-directed RNA polymerase (A) NSP7 (C), NSP8 (B, D) with sequence length of 942, 83, and 198 respectively. RNA-dependent RNA polymerase (RdRp) also known as NSP12 that catalyses the synthesis of viral RNA by associating with co-factors NSP7 and NSP8 thereby involves in viral replication and transcription of SARS-COV-2 genome. Currently, Remdesivir an antiviral drug in huge demand to treat moderate to severe n-Covid cases targets the viral polymerase NSP12 and hence this effort of molecular docking may shed some light on probable molecules to inhibit viral replication by interfering with NSP12 (Gao Y et al., 2020) (Figure 2).

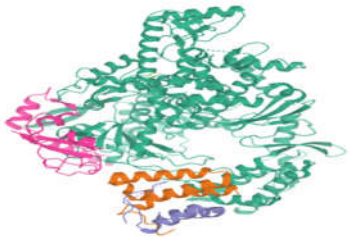

Figure 2: 3D view of 6M71 -SARS-CoV-2 RNA-dependent RNA polymerase in complex with cofactors

Targeting 3CL protease (6M2N)

6M2N is the X-ray crystallography structure of the 3CL protease (3CL pro) in complex with 5,6,7-trihydroxy-2-phenyl-4H-chromen-4-one, a novel inhibitor of SARS-CoV-2. The structure

composed of four chains A, B, C, and D, each of which is identified by a single sequence-unique entity with a total of 306 amino acids. Certain proteases like 3C-like protease (3CLpro), together with a papain-like protease (PLpro), enable to transform polypeptides into mature non structural proteins like RNA-dependent RNA polymerase (RdRp) and helicase, which are involved in essential for viral replication and maturation. These polyproteins contain 11 and 3 cleaving domains for PLpro and 3CLpro, respectively. Preferentially the substrate specificity of 3CLpro is highly conserved among different CoVs and is analogous to picornavirus 3C protease, thus rendering it an ideal target for the development of wide spectrum antiviral agents (Su HX et al., 2020) (Figure 3).

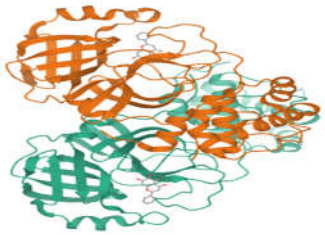

Figure 3: 3D view of 6M2N -SARS-CoV-2 3CL protease (3CL pro) in complex with a novel inhibitor

2.1.3 Drug library

Constructed the drug library with 86 phytoconstituents for the *in silico* molecular virtual docking (Table 3). Selected phytoconstituents downloaded from PubChem in structure data format (SDF) format.

2.1.4. Validation of X-crystal proteins of drug targets

The Ramachandran two-dimensional plot was used to validate the selected protein for using them in molecular docking studies. The plot represented favoured and disfavoured torsional angles - phi (φ) and psi (ψ) of amino acids in a protein/peptide.

2.1.5. Protein/Target preparation

In the glide protein preparation wizard, the proteins were directly imported into the workspace by entering their PDB codes 6M71, and 6M2N. Proteins pre-processed for assigning bond orders, adding hydrogen atoms, creating disulfide bonds, etc. In the review and modify tab, we selected the required chains to generate a receptor grid, followed by soaking the co-crystallized ligand in the protein, removing water molecules, and removing small molecules. In the refine tab, these proteins were optimized and minimized to their lowest energy state and proteins with a co-crystal ligand site chosen to screen the compounds' library.

2.1.6. Receptor grid generation

In Maestro's task window selected the receptor grid generation to make the grid active/binding site of the protein that is suitable for docking by choosing any one atom of the co-crystal ligand molecule. It displays a grid box with X, Y, and Z coordinates. For the protein 6M2N, the co-crystals is 5,6,7-trihydroxy-2-phenyl-4H-chromen-4-one, the workspace for grid formation. There is no valid co-crystal in the 3D structure of 6M71, so sitemap was used to identify the active site. As per sitemap, there were 5 active sites, and the top-ranked site was chosen for grid generation.

2.1.7. Ligand preparation

From the PubChem online database, imported the generated ligand library into Glide Schrodinger docking software 2019_4.3.1. Using glide ligprep, required parameters, including ionization, chirality, computation, etc., are assigned for the ligands from the workspace.

2.1.8. Ligand docking

Glide ligand docking was selected from tasks in Maestro, then the glide grid and ligand outmaegz zip files were loaded from the working directory. Through write XP descriptor settings, we virtually docked the compounds library.

2.1.9. Drug–likeness and ADME predictions:

The compounds are for further evaluated for drug-likeness using SwissADME: a free web application.

3. Results and discussion

Molecular docking

In this study, we virtually docked phytochemical constituents against two crystal structures of SARS-CoV-2 proteins that include: (i) the RNA dependent RNA polymerase (PDB ID: 6M71), (ii) 3CL protease (3CL pro) (PDB ID: 6M2N) by using the Glide Schrodinger docking software 2019_4. 3.1.

3.1. Molecular docking of Phyto principles to RNA dependent RNA polymerase (6M71)

In Coronaviridae, NSP12 encodes for RdRp, a highly crucial enzyme involved in viral genome replication and successful transcription and hence a potential drug target. The SARS-CoV-2 NSP12 domain contains a right hand RdRP domain, and a N-terminal extension domain which is unique to nidovirus. Th amino acid sequence of polymerase domain is highly conserved in viral polymerase family with additional three subdomains viz. a finger (L366-A581 and K621-G679), a palm (residues T582–P620 and T680–Q815) and a thumb sub-domain (H816–E920). The active site is formed in the palm domain by the highly conserved polymerase motifs (A–G).

The docking scores obtained from the docking of ligands with RNA-dependent RNA polymerase (NSP12) indicated that Scutellarein and Saikosaponin D as compounds with higher binding affinity with the binding energies -39.443and -43.588kcal/mol respectively, and corresponding docking scores were -7.252 and -5.381. The rest of the compounds showed very weak interaction with a score of less than -4.0. However, both Scutellarein and Saikosaponin D exhibited relatively less binding interaction than the reference ligands Remdesivir (-8.767) with binding energy of -54.744 kcal/mol. The analyses of amino acid interaction of ligands on the targets indicated that binding interaction of Scutellarein (H- bond interactions with THR 394, ASN 628and hydrophobic interaction with ARG 457) (Figure 6) and Saikosaponin D (H- bond interactions with THR 319, ILE 266, ASN 459 and hydrophobic interaction with PHE 396) (Figure 7) was quite satisfactory when compared to Remdesivir (H- bond interactions with TYR 89, GLY 165, SER 198 and hydrophobic interaction with LYS 90) (Figure 5).

Figure 4: Selected Phytochemicals used in current study.

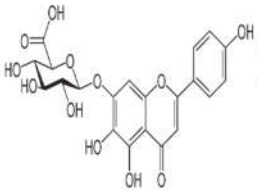

Scutellarein

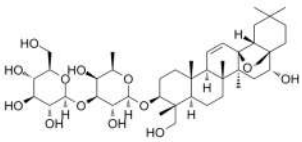

Saikosaponin D

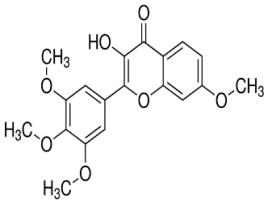

5-hydroxy-7,8,2',5'-tetramethoxyflavone

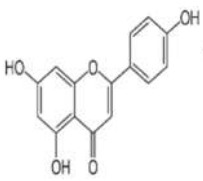

Apigenin

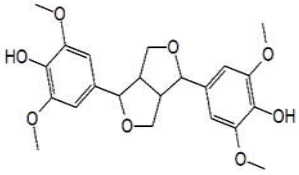

Syringaresinol

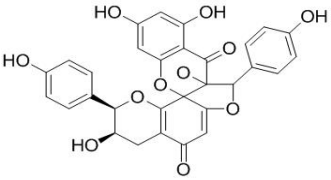

Stelleranol

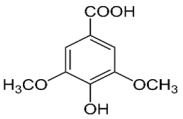

Syringic acid

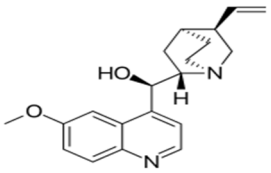

Quinine

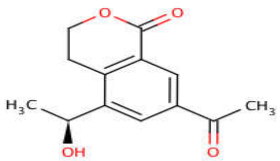

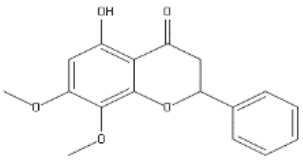

Swerilactone M7-O-methyldihydrowogonin

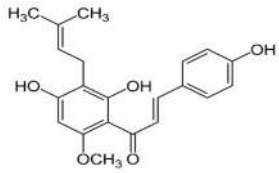

Roscovitin

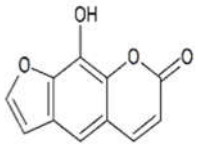

Rhinacanthin E

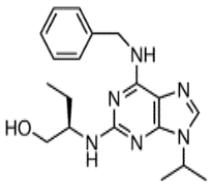

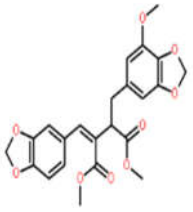

XanthohumolXanthtoxol

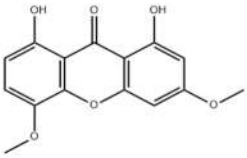

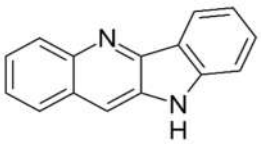

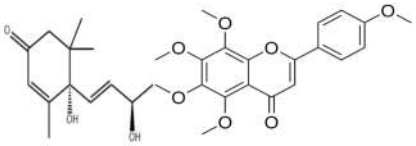

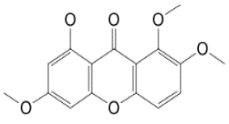

SwerchirinQuindoline **Sesquiterpene** **Tangeretin**

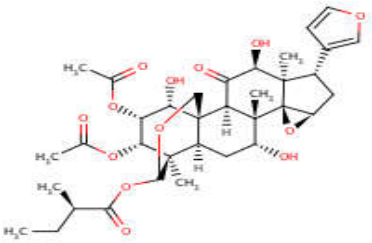

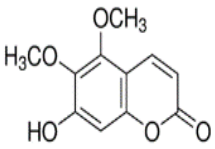

1-Hydroxy-3,7,8-trimethoxyxanthone **Trichilin AUmckalin**

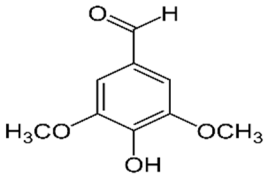

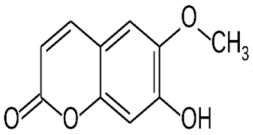

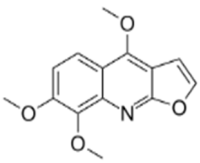

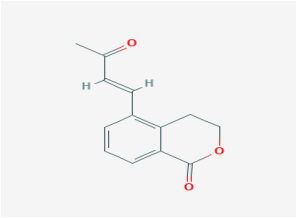

Syringaldehyde **ScopoletinSkimmianineSwerilactone O**

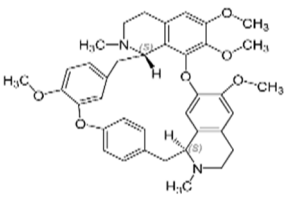

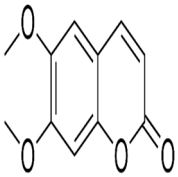

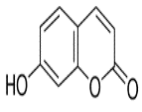

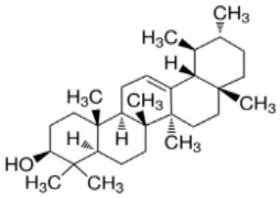

Tetrandrine Scoparone **Umbelliferone** **Alpha amyrin**

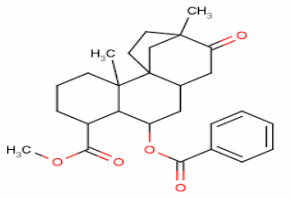

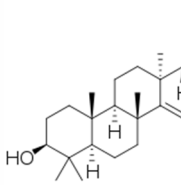

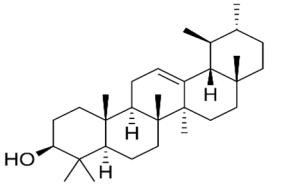

Scopadulcic acid B **Taraxerol** **β-Amyrin**

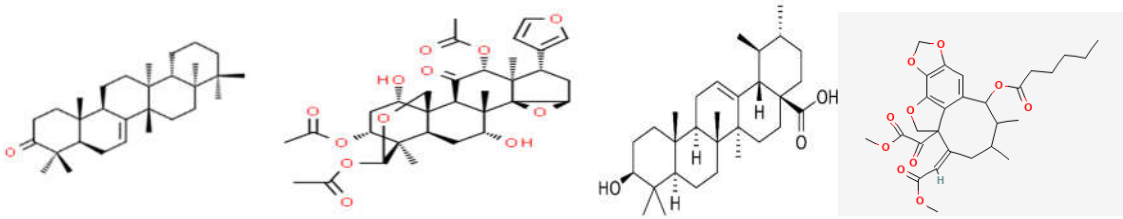

SendaninUrsolic acid Taiwanschirin Swertanone

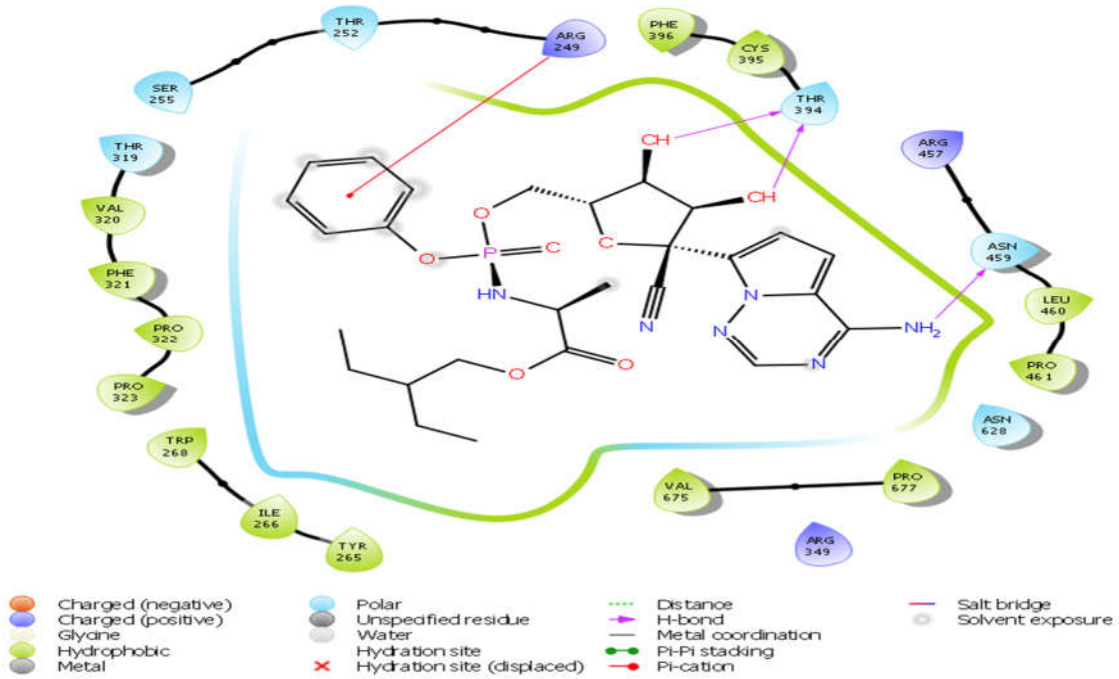

Figure 5: Remdesivir on 6M71

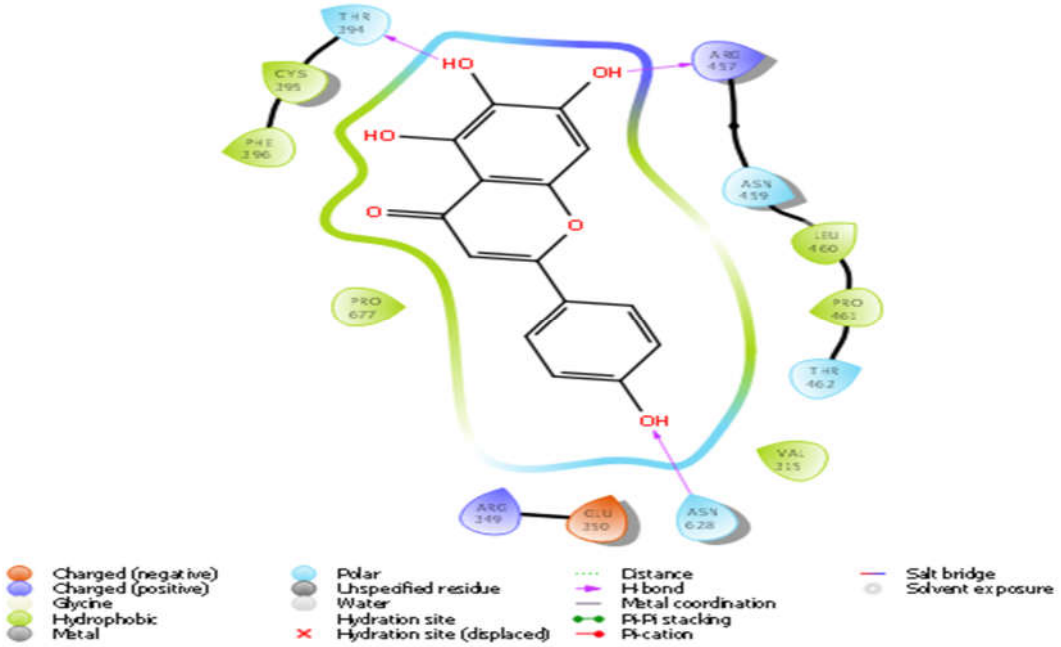

Figure 6: Scutellarein on 6M71

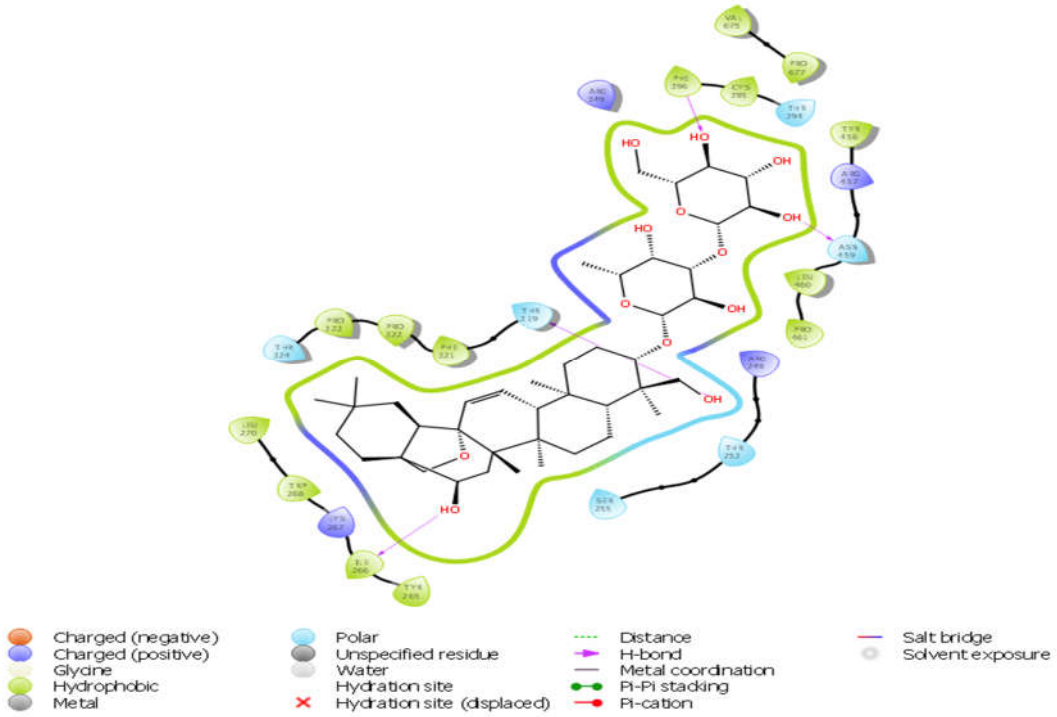

Figure 7: Saikosaponin on 6M71

Table 2: Docking results of selected Phytochemicals with RNA dependent RNA polymerase (PDB ID: 6M71):

CHEMICAL CONSTITUENTS	PUBCHEM ID	6M71	
		Glide score	Glide Energy
Scutellarein	5281697	-7.138	-39.443
Saikosaponin D	107793	-6.966	-43.588
5-Hydroxy-7,8,2',5'-tetramethoxyflavone	10948318	-5.967	-35.234
5,7,2',3-tetramethoxyflavone	181092	-5.676	-42.89
Apigenin	5280443	-5.546	-26.596
Trijugin A	101519185	-5.267	-32.632
Syringaresinol	100067	-5.041	-37.295
Stelleranol	131676072	-4.976	-47.487
Syringic acid	10742	-4.948	-27.819
Quinine	3034034	-4.825	-28.909
Swerilactone M	53483971	-4.729	-27.836
7-O-methyldihydrowogonin	13963770	-4.686	-32.67
Swerilactone N	53494394	-4.706	-24.053
Xanthohumol	639665	-4.518	-40.716
Rhinacanthin E	10366055	-4.438	-43.442
7-O-methylhydrowogonin	188316	-4.379	-35.305
Xanthtoxol	65090	-4.307	-20.476
Roscovitin	160355	-4.295	-34.73
Swerchirin	5281660	-4.184	-33.049
Quindoline	98912	-4.175	-24.839

Sesquiterpene	6473767	-3.712	-24.463
Schizarin B	10582671	-3.611	-41.136
1-Hydroxy-3,7,8-trimethoxyxanthone	5378284	-3.172	-29.101
Tangeretin	68077	-3.11	-36.484
Trichilins A	5462417	-0.765	-45.724
Umckalin	5316862	-3.784	-23.575
Syringaldehyde	8655	-4.136	-24.576
Scopoletin	5280460	0.167	-26.671
Skimmianine	6760	-3.16	-21.724
Swerilactone O	53494395	-3.572	-25.33
Tetrandrine	73078	--	-35.216
Scoparone	8417	-2.177	-23.263
Umbelliferone	5281426	-3.436	-17.706
Alpha amyrin	73170	-3.225	-32.777
Scopadulcic acid B	11729855	-2.746	-37.686
Taraxerol	92097	-3.193	-36.546
β-Amyrin	73145	-3.407	-31.55
Swertanone	102285187	-3.801	-31.792
Sendanin	5352038	-0.172	-40.341
Ursolic acid	64945	-3.751	-37.243
Taiwans chirin D	70697809	-3.385	-37.783

5.2. Molecular docking of phytoprinciples to 3CL protease (3CL pro) (6M2N)

Certain proteases like 3C-like protease (3CLpro), together with a papain-like protease (PLpro), enable to transform polypeptides into mature non-structural proteins like RNA-dependent RNA polymerase (RdRp) and helicase, which are involved in essential for viral replication and maturation. These polyproteins contain 11 and 3 cleaving domains for PLpro and 3CLpro, respectively. Preferentially, the substrate specificity of 3CLpro is highly conserved among different CoVs and is analogous to picornavirus 3C protease, thus rendering it an ideal target for the development of wide spectrum antiviral agents.

The docking scores of the docked ligands SARS-CoV-2 3CL protease (6M2N) showed that Syringaresinol and 5,7,2',3-Tetramethoxyflavone as compounds with higher binding affinity with the binding energies -45.203and -47.015kcal/mol respectively, and corresponding docking scores were -7.969and -7.453.Whilst the docking scores of co-crystalsBaicalein was found to be -7.552 with a binding energy of -42.537 kcal/mol. Other constituents, showed the docking scores about -7 with the binding energy ranged from -50 to -20 (Table 3). The analyses of amino acid interaction of ligands on the targets indicated that binding interaction of Syringaresinol (H- bonding with GLY143, GLU 166) (Figure 9) and 5,7,2',3-Tetramethoxy flavones (H- bonding with GLU 166, CYS 44, MET 49) (Figure 10) in comparison with standard Baicalein binding interactions (H-bonding with GLY 143 and GLU 166) (Figure 8).

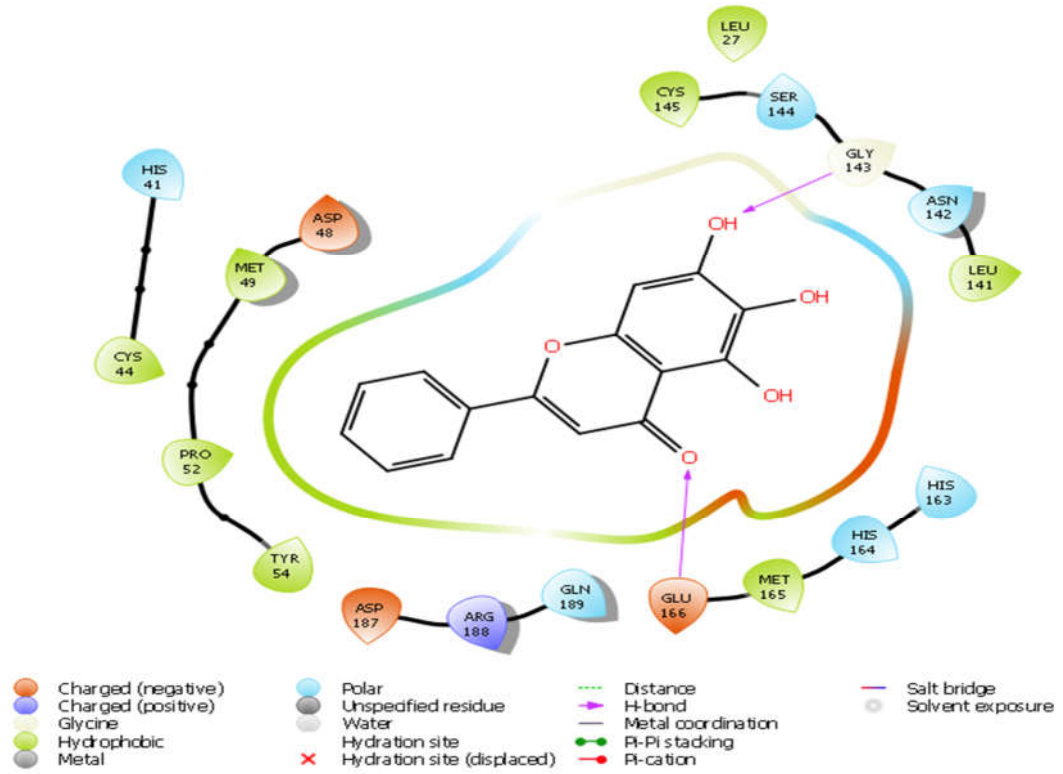

Figure 8:Baicalein on 6M2N

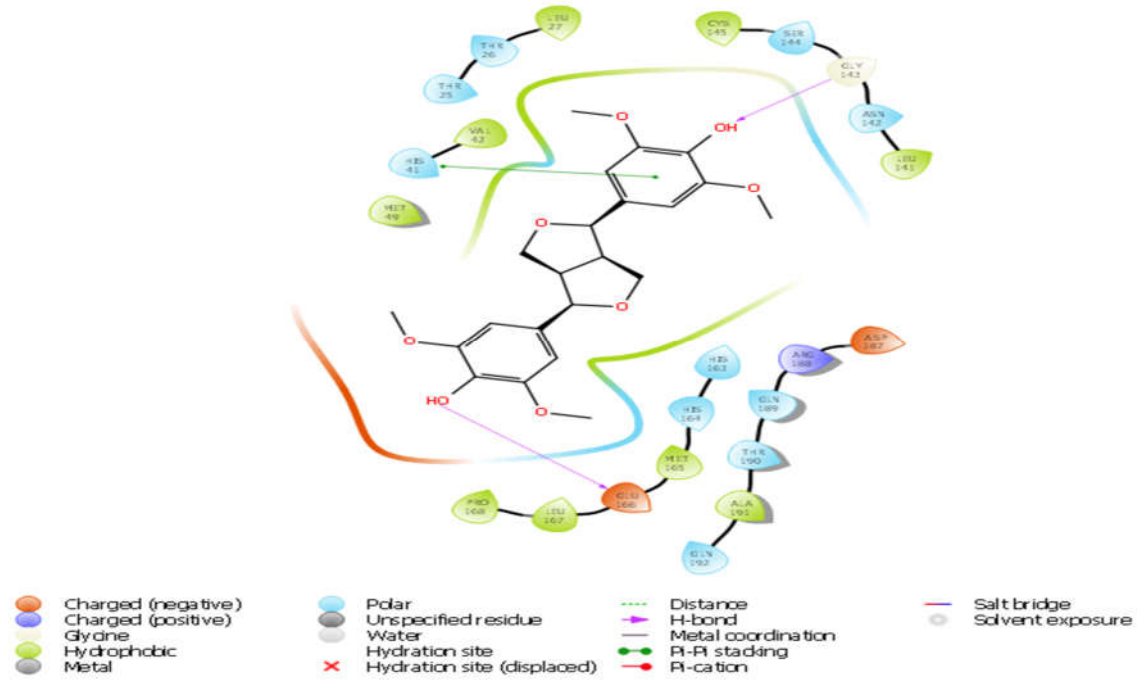

Figure 9:Syringaresinol on 6M2N

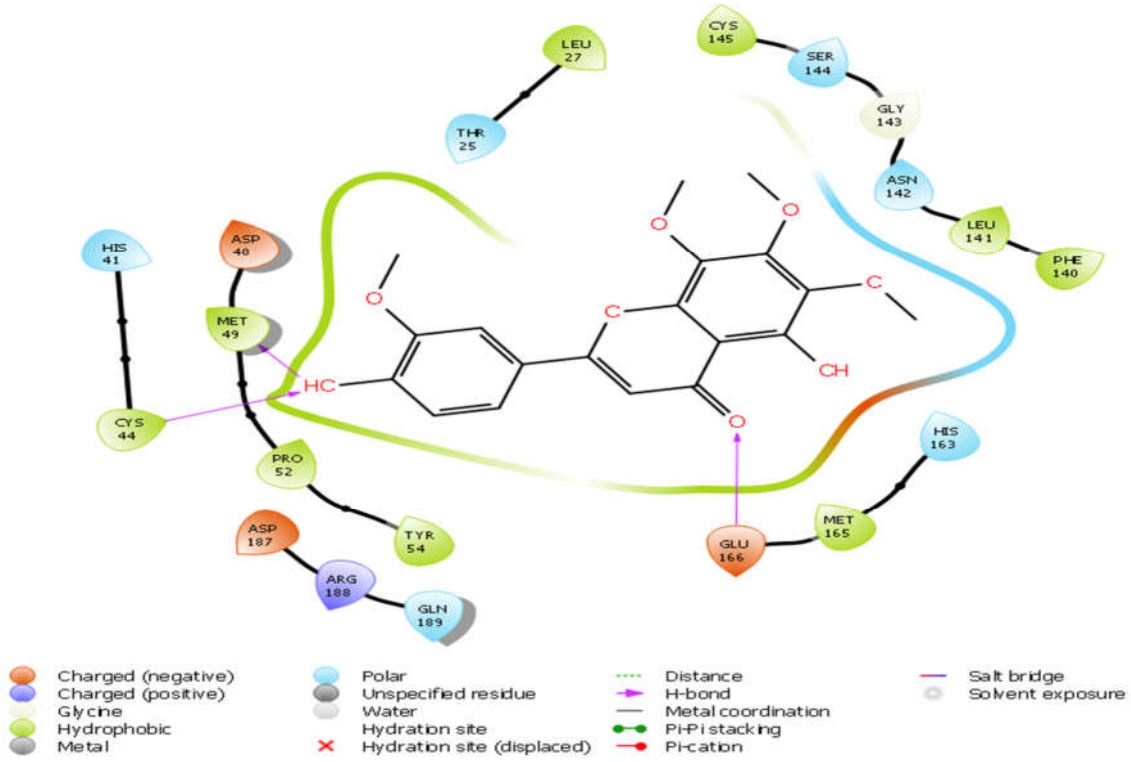

Figure 10: 5, 7, 2', 3-Tetramethoxyflavone on 6M2N

Table 3: Docking results of selected Phytochemicals with 3CL protease (3CL pro) (PDB ID: 6M2N):

Chemical constituents	Pubchem id	6M2N	
		Glide score	Glide energy
Syringaresinol	100067	-7.969	-45.203
5,7,2',3-Tetramethoxyflavone	181092	-7.453	-47.015
Apigenin	5280443	-7.421	-41.6
7-O-Methylhydrowogonin	188316	-6.97	-41.394
Swerchirin	5281660	-6.855	-40.713
5-Hydroxy-7,2',6'-trimethoxyflavone	5319878	-6.864	-50.801
Swerilactone	53494394	-6.658	-36.447
Narasin	65452	-6.475	-48.875
1-Hydroxy-3,7,8-trimethoxyxanthone	5378284	-6.414	-39.164
Roscovitin	160355	-6.389	-46.466

5.3. ADME Predictions of Phytoprinciples Using SwissADME

Finally, compounds with good binding affinity to the selected target further analyzed the drug ability using SwissADME: a free web tool.

5.3.1Results of ADME calculation

The most important and most difficult step in drug discovery and development (in which this account for the failure of about 60% of all drugs in the clinical phases) is carrying out DMPK (drug metabolism and pharmacokinetics) studies, often referred to as ADMET. In pharmacokinetic/pharmacology, ADME stands for “absorption, distribution, metabolism, and excretion”, in which they describe the disposition of a drug compound in the body. ADME Predictor is a designed program of a computer for estimating pharmacokinetic parameters/properties of drug-like compounds from their molecular structures called the ADME (Singh et al., 2013). Swiss ADME web tool is freely available software utilized to predict the physicochemical properties, absorption, distribution, metabolism, elimination and pharmacokinetic properties of molecules, which are key determinants for more clinical trials. It takes into account six physico-chemical properties, which are very vital, like lipophilicity, flexibility, saturation, polarity, solubility, and size. The result of the ADME revealed physicochemical properties of the designed compounds which includes the rules of five (MW, iLOGP, HBAs and HBDs) and several other parameters/properties like molecular polar surface area (TPSA), number of rotatable bonds (ROTBs), number of aromatic heavy atoms, and number of alerts for undesirable substructures (i.e., PAINS #alert and Brenk #alert), among others as represented in the Table 4 below. Molecular weight (MW), number of rotatable bonds (RB), number of hydrogen donors (HBD), number of hydrogen acceptors (HBA), Topo-logical Polar Surface Area (TPSA), octanol/water partition coefficient (iLOGP), number of aromatic heavy atoms (nAH), Molar refractivity(MR) and the number of alerts for undesirable substructures/sub-structures (Brenk #alert and PAINS #alert) are presented in Table 4.According to Lipinski's rule of five and the concept of QED as presented in Table 4, all the docked compounds were in accordance with the rules by causing no more than one violation. That is to say, all the MW, RB, HBD, HBA, TPSA, iLOGP, nAH and MR are within the acceptable range. Almost, 14 compounds possess a good pharmacokinetic profile with high BBB penetration presented in Table 4.

Table 4: Physicochemical properties and ADME properties of selected Phytochemicals:

Molecule	Formula	MW	#Heavy atoms	#Aromatic heavy atoms	Fraction Csp3	#Rotatable bonds	#H-bond acceptors	#H-bond donors	MR	TPSA	iLOGP	XLOGP3	WLOGP	MLOGP	Silicos-IT Log P	Consensus Log P	ESOL Log S	ESOL Solubility (mg/ml)	ESOL Solubility (mol/l)
Scutellarein	C42H68O13	780.98	55	0	0.95	6	13	8	199.82	207.99	3.28	2.52	1.78	0.18	1.14	1.78	-5.87	1.04E-03	1.34E-06
Saikosaponin D	C19H18O7	358.34	26	16	0.21	5	7	1	95.91	87.36	3.6	3.26	3.2	0.4	3.66	2.83	-4.24	2.06E-02	5.74E-05
5-hydroxy-7,8,2',5'-tetramethoxyflavone	C15H10O5	270.24	20	16	0	1	5	3	73.99	90.9	1.89	3.02	2.58	0.52	2.52	2.11	-3.94	3.07E-02	1.14E-04
Apigenin	C22H34O6	394.5	28	0	0.73	6	6	1	107.55	85.36	3.66	3.18	3.33	2.33	3.18	3.14	-3.89	5.04E-02	1.28E-04
Trijugin A	C30H22O11	558.49	41	18	0.2	2	11	6	138.82	183.21	2.24	1.68	1.92	-0.92	1.79	1.34	-4.55	1.56E-02	2.79E-05
Syringaresinol	C9H10O5	198.17	14	6	0.22	3	5	2	48.41	75.99	1.54	1.04	1.11	0.49	0.77	0.99	-1.84	2.84E+00	1.44E-02
Stelleranol	C20H24N2O2	324.42	24	10	0.45	4	4	1	99.73	45.59	3.36	2.88	2.47	2.23	3.11	2.81	-3.71	6.32E-02	1.95E-04
Syringic acid	C13H14O4	234.25	17	6	0.38	2	4	1	61.7	63.6	1.88	1.01	1.33	1.19	2.78	1.64	-2.06	2.05E+00	8.75E-03
Quinine	C16H12O5	284.26	21	16	0.06	2	5	2	78.46	79.9	2.55	3.49	2.88	0.77	3.03	2.54	-4.23	1.66E-02	5.85E-05
Swerilactone M	C13H14O4	234.25	17	6	0.38	3	4	1	61.32	63.6	1.92	0.61	1.09	1.19	2.65	1.49	-1.74	4.26E+00	1.82E-02
7-0-methyldihydrowogonin	C21H22O5	354.4	26	12	0.19	6	5	3	102.53	86.99	2.93	5.07	4.11	2.36	4.31	3.76	-5.18	2.36E-03	6.65E-06
Swerilactone N	C23H22O9	442.42	32	12	0.3	9	9	0	111.05	98.75	3.86	3.59	2.63	1.93	4.04	3.21	-4.53	1.31E-02	2.96E-05
Xanthohumol	C19H26N6O	354.45	26	15	0.42	8	4	3	104.88	87.89	3.03	3.16	2.67	1.61	2.09	2.51	-3.93	4.19E-02	1.18E-04
Rhinacanthin E	C15H12O6	288.25	21	14	0.13	2	6	2	77.02	89.13	2.9	2.75	2.37	0.28	2.52	2.16	-3.72	5.48E-02	1.90E-04
Xanthtoxol	C15H10N2	218.25	17	17	0	0	1	1	71.11	28.68	2.02	3.74	3.87	3.04	4.05	3.35	-4.29	1.12E-02	5.14E-05
Roscovitin	C30H34O13	602.58	43	0	0.8	2	13	3	137.29	190.95	2.65	-0.3	-0.93	0.09	0.71	0.44	-3.26	3.35E-01	5.56E-04
Swerchirin	C27H34O8	486.55	35	12	0.52	7	8	1	131.81	92.68	4.05	5.66	4.95	2.73	5	4.48	-6.21	2.97E-04	6.11E-07
Quindoline	C16H14O6	302.28	22	14	0.19	3	6	1	81.49	78.13	2.97	3.07	2.68	0.53	3.04	2.46	-3.92	3.62E-02	1.20E-04
Sesquiterpene	C20H20O7	372.37	27	16	0.25	6	7	0	100.38	76.36	3.71	3.04	3.5	0.63	4.21	3.02	-4.11	2.91E-02	7.83E-05
Schizarin B	C35H46O13	674.73	48	5	0.77	9	13	3	163.91	191.56	3.98	1.67	2.03	0.49	2.65	2.16	-4.56	1.86E-02	2.76E-05
1-Hydroxy-3,7,8- trimethoxyxanthone	C11H10O5	222.19	16	10	0.18	2	5	1	57.49	68.9	2.13	1.5	1.52	0.49	1.94	1.51	-2.49	7.14E-01	3.21E-03
Tangeretin	C9H10O4	182.17	13	6	0.22	3	4	1	46.84	55.76	1.66	-0.01	1.22	0.24	1.51	0.93	-1.11	1.42E+01	7.82E-02
Trichilin A	C10H8O4	192.17	14	10	0.1	1	4	1	51	59.67	1.86	1.53	1.51	0.76	1.94	1.52	-2.46	6.70E-01	3.48E-03
Umckalin	C14H13NO4	259.26	19	13	0.21	3	5	0	70.99	53.72	2.78	2.84	3.01	1.09	2.9	2.52	-3.54	7.39E-02	2.85E-04
Syringaldehyde	C13H12O3	216.23	16	6	0.23	2	3	0	60.48	43.37	2.03	1.92	1.89	1.96	3.25	2.21	-2.54	6.30E-01	2.91E-03
Scopoletin	C38H42N2O6	622.75	46	24	0.37	4	8	0	186.07	61.86	4.87	6.66	5.75	3.73	6.06	5.41	-8.02	5.96E-06	9.57E-09
Skimmianine	C11H10O4	206.19	15	10	0.18	2	4	0	55.47	48.67	2.23	1.71	1.81	1.05	2.42	1.84	-2.56	5.72E-01	2.77E-03
Swerilactone O	C9H6O3	162.14	12	10	0	0	3	1	44.51	50.44	1.44	1.58	1.5	1.04	1.97	1.51	-2.46	5.66E-01	3.49E-03
Tetrandrine	C30H50O	426.72	31	0	0.93	0	1	1	135.14	20.23	4.77	9.01	8.02	6.92	6.52	7.05	-8.16	2.94E-06	6.89E-09
Scoparone	C27H34O5	438.56	32	6	0.67	4	5	1	121.53	80.67	3.18	5.24	5.28	4.28	4.82	4.56	-5.73	8.07E-04	1.84E-06
Umbelliferone	C30H50O	426.72	31	0	0.93	0	1	1	134.88	20.23	4.77	9.3	8.17	6.92	6.92	7.22	-8.34	1.93E-06	4.52E-09
Alpha amyrin	C30H50O	426.72	31	0	0.93	0	1	1	134.88	20.23	4.74	9.15	8.17	6.92	6.92	7.18	-8.25	2.40E-06	5.62E-09
Scopadulcic acid B	C30H48O	424.7	31	0	0.9	0	1	0	133.92	17.07	4.47	8.84	8.38	6.82	7.51	7.2	-8.04	3.85E-06	9.07E-09
Taraxerol	C32H40O12	616.65	44	5	0.75	7	12	2	148.33	171.33	3.35	1.25	2.04	0.69	2.46	1.96	-4.07	5.21E-02	8.46E-05
β-Amyrin	C30H48O3	456.7	33	0	0.9	1	3	2	136.91	57.53	3.71	7.34	7.09	5.82	5.46	5.88	-7.23	2.69E-05	5.89E-08
Swertanone	C28H34O10	530.56	38	6	0.57	11	10	0	134.69	123.66	4.42	4.2	3.4	2.13	4.9	3.81	-5.17	3.62E-03	6.82E-06
Sendanin	C14H13NO4	259.26	19	13	0.21	3	5	0	70.99	53.72	2.78	2.84	3.01	1.09	2.9	2.52	-3.54	7.39E-02	2.85E-04
Ursolic acid	C13H12O3	216.23	16	6	0.23	2	3	0	60.48	43.37	2.03	1.92	1.89	1.96	3.25	2.21	-2.54	6.30E-01	2.91E-03
Taiwanschirin D	C28H34O10	530.56	38	6	0.57	11	10	0	134.69	123.66	4.42	4.2	3.4	2.13	4.9	3.81	-5.17	3.62E-03	6.82E-06

Molecule	Formula	MW	ESOL Class	Ali Log S	Ali Solubility (mg/ml)	Ali Solubility (mol/l)	Ali Class	Silicos-IT LogSw	Silicos-IT Solubility (mg/ml)	Silicos-IT Solubility (mol/l)	Silicos-IT class	GI absorption	BBB permeant	Pgp substrate	CYP1A2 inhibitor	CYP2C19 inhibitor	CYP2C9 inhibitor	CYP2D6 inhibitor	CYP3A4 inhibitor
Scutellarein	C42H68O13	780.98	Moderately soluble	-6.53	2.28E-04	2.92E-07	Poorly soluble	-2.08	6.50E+00	8.32E-03	Soluble	Low	No	Yes	No	No	No	No	No
Saikosaponin D	C19H18O7	358.34	Moderately soluble	-4.77	6.10E-03	1.70E-05	Moderately soluble	-6.02	3.43E-04	9.57E-07	Poorly soluble	High	No	No	Yes	No	Yes	Yes	Yes
5-hydroxy-7,8,2',5'-tetramethoxyflavone	C15H10O5	270.24	Soluble	-4.59	6.88E-03	2.55E-05	Moderately soluble	-4.4	1.07E-02	3.94E-05	Moderately soluble	High	No	No	Yes	No	No	Yes	Yes
Apigenin	C22H34O6	394.5	Soluble	-4.64	8.96E-03	2.27E-05	Moderately soluble	-2.56	1.08E+00	2.74E-03	Soluble	High	No	No	No	No	No	No	Yes
Trijugin A	C30H22O11	558.49	Moderately soluble	-5.14	4.03E-03	7.21E-06	Moderately soluble	-5.06	4.86E-03	8.71E-06	Moderately soluble	Low	No	No	No	No	Yes	No	No
Syringaresinol	C9H10O5	198.17	Very soluble	-2.23	1.18E+00	5.94E-03	Soluble	-1.46	6.93E+00	3.50E-02	Soluble	High	No	No	No	No	No	No	No
Stelleranol	C20H24N2O2	324.42	Soluble	-3.5	1.03E-01	3.18E-04	Soluble	-4.31	1.60E-02	4.92E-05	Moderately soluble	High	Yes	No	No	No	No	Yes	No
Syringic acid	C13H14O4	234.25	Soluble	-1.93	2.72E+00	1.16E-02	Very soluble	-3.06	2.04E-01	8.69E-04	Soluble	High	Yes	No	No	No	No	No	No
Quinine	C16H12O5	284.26	Moderately soluble	-4.85	4.01E-03	1.41E-05	Moderately soluble	-5.1	2.25E-03	7.91E-06	Moderately soluble	High	No	No	Yes	No	Yes	Yes	Yes
Swerilactone M	C13H14O4	234.25	Very soluble	-1.52	7.08E+00	3.02E-02	Very soluble	-3.08	1.96E-01	8.36E-04	Soluble	High	Yes	No	No	No	No	No	No
7-O-methyldihydrowogonin	C21H22O5	354.4	Moderately soluble	-6.64	8.14E-05	2.30E-07	Poorly soluble	-4.58	9.26E-03	2.61E-05	Moderately soluble	High	No	No	Yes	No	Yes	No	Yes
Swerilactone N	C23H22O9	442.42	Moderately soluble	-5.35	1.97E-03	4.46E-06	Moderately soluble	-5.13	3.30E-03	7.46E-06	Moderately soluble	High	No	No	Yes	Yes	Yes	No	Yes
Xanthohumol	C19H26N6O	354.45	Soluble	-4.68	7.47E-03	2.11E-05	Moderately soluble	-5.82	5.40E-04	1.52E-06	Moderately soluble	High	No	Yes	Yes	No	No	Yes	Yes
Rhinacanthin E	C15H12O6	288.25	Soluble	-4.28	1.52E-02	5.29E-05	Moderately soluble	-4.39	1.18E-02	4.10E-05	Moderately soluble	High	No	No	Yes	No	Yes	Yes	Yes
Xanthtoxol	C15H10N2	218.25	Moderately soluble	-4.03	2.02E-02	9.24E-05	Moderately soluble	-6.27	1.17E-04	5.38E-07	Poorly soluble	High	Yes	Yes	Yes	No	No	Yes	Yes
Roscovitin	C30H34O13	602.58	Soluble	-3.25	3.39E-01	5.63E-04	Soluble	-0.77	1.02E+02	1.69E-01	Soluble	Low	No	Yes	No	No	No	No	No
Swerchirin	C27H34O8	486.55	Poorly soluble	-7.37	2.07E-05	4.26E-08	Poorly soluble	-6.42	1.85E-04	3.79E-07	Poorly soluble	High	No	No	No	No	No	No	No
Quindoline	C16H14O6	302.28	Soluble	-4.38	1.27E-02	4.19E-05	Moderately soluble	-5.08	2.49E-03	8.24E-06	Moderately soluble	High	Yes	No	Yes	No	Yes	Yes	Yes
Sesquiterpene	C20H20O7	372.37	Moderately soluble	-4.31	1.83E-02	4.90E-05	Moderately soluble	-6.71	7.24E-05	1.95E-07	Poorly soluble	High	Yes	No	No	No	Yes	No	Yes
Schizarin B	C35H46O13	674.73	Moderately soluble	-5.31	3.33E-03	4.93E-06	Moderately soluble	-3.98	7.10E-02	1.05E-04	Soluble	Low	No	Yes	No	No	No	No	No
1-Hydroxy-3,7,8- trimethoxyxanthone	C11H10O5	222.19	Soluble	-2.55	6.20E-01	2.79E-03	Soluble	-3.3	1.12E-01	5.02E-04	Soluble	High	Yes	No	Yes	No	No	No	No
Tangeretin	C9H10O4	182.17	Very soluble	-0.71	3.54E+01	1.94E-01	Very soluble	-2.03	1.72E+00	9.42E-03	Soluble	High	Yes	No	No	No	No	No	No
Trichilin A	C10H8O4	192.17	Soluble	-2.39	7.79E-01	4.06E-03	Soluble	-3.17	1.31E-01	6.81E-04	Soluble	High	Yes	No	Yes	No	No	No	No
Umckalin	C14H13NO4	259.26	Soluble	-3.63	6.13E-02	2.36E-04	Soluble	-4.98	2.73E-03	1.05E-05	Moderately soluble	High	Yes	No	Yes	Yes	Yes	Yes	Yes
Syringaldehyde	C13H12O3	216.23	Soluble	-2.45	7.60E-01	3.51E-03	Soluble	-3.29	1.11E-01	5.14E-04	Soluble	High	Yes	No	Yes	No	No	No	No
Scopoletin	C38H42N2O6	622.75	Poorly soluble	-7.76	1.08E-05	1.73E-08	Poorly soluble	-10.8	9.78E-09	1.57E-11	Insoluble	High	No	No	No	No	No	No	No
Skimmianine	C11H10O4	206.19	Soluble	-2.35	9.26E-01	4.49E-03	Soluble	-3.87	2.76E-02	1.34E-04	Soluble	High	Yes	No	Yes	No	No	No	No
Swerilactone O	C9H6O3	162.14	Soluble	-2.25	9.12E-01	5.62E-03	Soluble	-3.03	1.53E-01	9.42E-04	Soluble	High	Yes	No	Yes	No	No	No	No
Tetrandrine	C30H50O	426.72	Poorly soluble	-9.33	2.02E-07	4.72E-10	Poorly soluble	-6.71	8.23E-05	1.93E-07	Poorly soluble	Low	No	No	No	No	No	No	No
Scoparone	C27H34O5	438.56	Moderately soluble	-6.68	9.10E-05	2.08E-07	Poorly soluble	-6.1	3.52E-04	8.02E-07	Poorly soluble	High	No	Yes	No	No	Yes	No	Yes
Umbelliferone	C30H50O	426.72	Poorly soluble	-9.63	1.01E-07	2.36E-10	Poorly soluble	-7.16	2.93E-05	6.85E-08	Poorly soluble	Low	No	No	No	No	No	No	No
Alpha amyrin	C30H50O	426.72	Poorly soluble	-9.47	1.44E-07	3.38E-10	Poorly soluble	-7.16	2.93E-05	6.85E-08	Poorly soluble	Low	No	No	No	No	No	No	No
Scopadulcic acid B	C30H48O	424.7	Poorly soluble	-9.08	3.51E-07	8.26E-10	Poorly soluble	-7.86	5.86E-06	1.38E-08	Poorly soluble	Low	No	No	No	No	No	No	No
Taraxerol	C32H40O12	616.65	Moderately soluble	-4.45	2.21E-02	3.58E-05	Moderately soluble	-4.03	5.82E-02	9.44E-05	Moderately soluble	Low	No	Yes	No	No	No	Yes	No
β-Amyrin	C30H48O3	456.7	Poorly soluble	-8.38	1.92E-06	4.21E-09	Poorly soluble	-5.67	9.72E-04	2.13E-06	Moderately soluble	Low	No	No	No	No	No	No	No
Swertanone	C28H34O10	530.56	Moderately soluble	-6.51	1.65E-04	3.12E-07	Poorly soluble	-5.51	1.62E-03	3.05E-06	Moderately soluble	High	No	No	No	No	Yes	Yes	Yes
Sendanin	C14H13NO4	259.26	Soluble	-3.63	6.13E-02	2.36E-04	Soluble	-4.98	2.73E-03	1.05E-05	Moderately soluble	High	Yes	No	Yes	Yes	Yes	Yes	Yes
Ursolic acid	C13H12O3	216.23	Soluble	-2.45	7.60E-01	3.51E-03	Soluble	-3.29	1.11E-01	5.14E-04	Soluble	High	Yes	No	Yes	No	No	No	No
Taiwanschirin D	C28H34O10	530.56	Moderately soluble	-6.51	1.65E-04	3.12E-07	Poorly soluble	-5.51	1.62E-03	3.05E-06	Moderately soluble	High	No	No	No	No	Yes	Yes	Yes

4. SUMMARY &CONCLUSION

In present work, the possible anti-nCOVID potential of phytochemicals were tested and analyzed through in silico methods. The docking studies pointed out the possible lead-like properties to some phytoconstituents and were validated as having drug like nature. This library was considered for tackling the modern-day issue of SARS-CoV-2 and further tested against the RNA dependent RNA polymerase (RdRp)and 3CL protease (3CL pro) key viral proteins. Analysis of protein-ligand docking revealed the following: the phytochemicals/bioactives such as Scutellarein, Saikosaponin D, Syringaresinol and 5,7,2',3-Tetramethoxyflavone hold promise in inhibiting the SARS-CoV-2 key viral proteins. The selected phytochemicals displayed the capability to suppress SARS-CoV-2 proteins and justify their further in vitro and in vivo studies. The present study could be the starting point for the future ligands from natural sources in 2019-nCoV RdRp and 3CL pro.

REFERENCES

1.Ji W, Wang W, Zhao X, Zai J, Li X. Cross-species transmission of the newly identified coronavirus 2019-nCoV. Journal of medical virology. 2020 Apr;92(4):433-40.

2.Wu JT, Leung K, Leung GM. Nowcasting and forecasting the potential domestic and international spread of the 2019-nCoV outbreak originating in Wuhan, China: a modelling study. The Lancet. 2020 Feb 29;395(10225):689-97.

3.Arya A, Dwivedi VD. Synergistic effect of Vitamin D and Remdesivir can fight COVID-19. Journal of Biomolecular Structure and Dynamics. 2020 Jun 8:1-2.

4.Beura S, Chetti P. In-silico strategies for probing chloroquine-based inhibitors against SARS-CoV-2. Journal of Biomolecular Structure and Dynamics. 2020 Jun 4:1-3.

5.Kumar A, Choudhir G, Shukla SK, Sharma M, Tyagi P, Bhushan A, Rathore M. Identification of phytochemical inhibitors against main protease of COVID-19 using molecular modeling approaches. Journal of Biomolecular Structure and Dynamics. 2020 Jun 2:1-1.

6.Mahanta S, Chowdhury P, Gogoi N, Goswami N, Borah D, Kumar R, Chetia D, Borah P, Buragohain AK, Gogoi B. Potential anti-viral activity of approved repurposed drug against main protease of SARS-CoV-2: an in silico-based approach. Journal of Biomolecular Structure and Dynamics. 2020 May 22:1-0.

7.Jauregui AR, Savalia D, Lowry VK, Farrell CM, Wathelet MG. Identification of residues of SARS-CoV nsp1 that differentially affect inhibition of gene expression and antiviral signaling. PloS one. 2013 Apr 29;8(4): e62416.

8.Cornillez-Ty CT, Liao L, Yates JR, Kuhn P, Buchmeier MJ. Severe acute respiratory syndrome coronavirus nonstructural protein 2 interacts with a host protein complex involved in mitochondrial biogenesis and intracellular signaling. Journal of virology. 2009 Oct 1;83(19):10314-8.

9.Z. Lab. Genome-wide structure and function modeling of SARS-CoV 2, https://zhanglab.ccmb.med.umich.edu/covid-19/, 2020.

10.Báez-Santos YM, John SE, Mesecar AD. The SARS-coronavirus papain-like protease: structure, function and inhibition by designed antiviral compounds. Antiviral research. 2015 Mar 1; 115:21-38.

11.Michalska K, Kim Y, Jedrzejczak R, Maltseva NI, Stols L, Endres M, Joachimiak A. Crystal structures of SARS-CoV-2 ADP-ribose phosphatase: from the apo form to ligand complexes. IUCrJ. 2020 Sep 1;7(5).

12.Sakai Y, Kawachi K, Terada Y, Omori H, Matsuura Y, Kamitani W. Two-amino acids change in the nsp4 of SARS coronavirus abolishes viral replication. Virology. 2017 Oct 1; 510:165-74.

13.Jumper J, Tunyasuvunakool K, Kohli P, Hassabis D. the AlphaFold team. Computational predictions of protein structures associated with COVID-19, version. 2020 Mar 5;2.

14.Wu C, Liu Y, Yang Y, Zhang P, Zhong W, Wang Y, Wang Q, Xu Y, Li M, Li X, Zheng M. Analysis of therapeutic targets for SARS-CoV-2 and discovery of potential drugs by computational methods. Acta Pharmaceutica Sinica B. 2020 May 1;10(5):766-88.

15.Douangamath A, Fearon D, Gehrtz P, Krojer T, Lukacik P, Owen CD, Resnick E, Strain-Damerell C, Aimon A, Ábrányi-Balogh P, Brandão-Neto J. Crystallographic and electrophilic fragment screening of the SARS-CoV-2 main protease. Nature communications. 2020 Oct 7;11(1):1-1.

16.Angelini MM, Akhlaghpour M, Neuman BW, Buchmeier MJ. Severe acute respiratory syndrome coronavirus nonstructural proteins 3, 4, and 6 induce double-membrane vesicles. MBio. 2013 Aug 30;4(4).

17.Cottam EM, Whelband MC, Wileman T. Coronavirus NSP6 restricts autophagosome expansion. Autophagy. 2014 Aug 20;10(8):1426-41.

18.Kirchdoerfer RN, Ward AB. Structure of the SARS-CoV nsp12 polymerase bound to nsp7 and nsp8 co-factors. Nature communications. 2019 May 28;10(1):1-9.

19.Snijder EJ, Decroly E, Ziebuhr J. The nonstructural proteins directing coronavirus RNA synthesis and processing. Advances in virus research. 2016 Jan 1; 96:59-126.

20.Rogstam A, Nyblom M, Christensen S, Sele C, Talibov VO, Lindvall T, Rasmussen AA, André I, Fisher Z, Knecht W, Kozielski F. Crystal Structure of Non-Structural Protein 10 from Severe Acute Respiratory Syndrome Coronavirus-2. International journal of molecular sciences. 2020 Jan;21(19):7375.

21.Gao Y, Yan L, Huang Y, Liu F, Zhao Y, Cao L, Wang T, Sun Q, Ming Z, Zhang L, Ge J. Structure of the RNA-dependent RNA polymerase from COVID-19 virus. Science. 2020 May 15;368(6492):779-82.

21.Jang KJ, Jeong S, Kang DY, Sp N, Yang YM, Kim DE. A high ATP concentration enhances the cooperative translocation of the SARS coronavirus helicase nsP13 in the unwinding of duplex RNA. Scientific reports. 2020 Mar 11;10(1):1-3.

22.Ferron F, Subissi L, De Morais AT, Le NT, Sevajol M, Gluais L, Decroly E, Vonrhein C, Bricogne G, Canard B, Imbert I. Structural and molecular basis of mismatch correction and ribavirin excision from coronavirus RNA. Proceedings of the National Academy of Sciences. 2018 Jan 9;115(2): E162-71.

23.Deng X, Hackbart M, Mettelman RC, O'Brien A, Mielech AM, Yi G, Kao CC, Baker SC. Coronavirus nonstructural protein 15 mediates evasion of dsRNA sensors and limits apoptosis in macrophages. Proceedings of the National Academy of Sciences. 2017 May 23;114(21): E4251-60.

24.Rosas-Lemus M, Minasov G, Shuvalova L, Inniss NL, Kiryukhina O, Wiersum G, Kim Y, Jedrzejczak R, Maltseva NI, Endres M, Jaroszewski L. The crystal structure of nsp10-nsp16 heterodimer from SARS-CoV-2 in complex with S-adenosylmethionine. bioRxiv. 2020 Apr 26.

25.Hoffmann M, Kleine-Weber H, Schroeder S, Krüger N, Herrler T, Erichsen S, Schiergens TS, Herrler G, Wu NH, Nitsche A, Müller MA. SARS-CoV-2 cell entry depends on ACE2 and TMPRSS2 and is blocked by a clinically proven protease inhibitor. cell. 2020 Apr 16;181(2):271-80.

26.Chi X, Yan R, Zhang J, Zhang G, Zhang Y, Hao M, Zhang Z, Fan P, Dong Y, Yang Y, Chen Z. A neutralizing human antibody binds to the N-terminal domain of the Spike protein of SARS-CoV-2. Science. 2020 Aug 7;369(6504):650-5.

27.Siu KL, Yuen KS, Castano-Rodriguez C, Ye ZW, Yeung ML, Fung SY, Yuan S, Chan CP, Yuen KY, Enjuanes L, Jin DY. Severe acute respiratory syndrome Coronavirus ORF3a protein activates the NLRP3 inflammasome by promoting TRAF3-dependent ubiquitination of ASC. The FASEB Journal. 2019 Aug;33(8):8865-77.
28.Kern DM, Sorum B, Mali SS, Hoel CM, Sridharan S, Remis JP, Toso DB, Kotecha A, Bautista DM, Brohawn SG. Cryo-EM structure of the SARS-CoV-2 3a ion channel in lipid nanodiscs. BioRxiv. 2020 Jan 1.
29.Kamau A, Kulmanov M, Arold ST, Pain A, Gojobori T, Duarte CM. Functional pangenome analysis suggests inhibition of the protein E as a readily available therapy for COVID-2019. bioRxiv. 2020 Jan 1.
30.Schoeman D, Fielding BC. Coronavirus envelope protein: current knowledge. Virology journal. 2019 Dec;16(1):1-22.
31.Mandala VS, McKay MJ, Shcherbakov AA, Dregni AJ, Kolocouris A, Hong M. Structure and drug binding of the SARS-CoV-2 envelope protein transmembrane domain in lipid bilayers. Nature Structural & Molecular Biology. 2020 Dec;27(12):1202-8.
32.Voß D, Pfefferle S, Drosten C, Stevermann L, Traggiai E, Lanzavecchia A, Becker S. Studies on membrane topology, N-glycosylation and functionality of SARS-CoV membrane protein. Virology journal. 2009 Dec;6(1):1-3.
33.Huang SH, Lee TY, Lin YJ, Wan L, Lai CH, Lin CW. Phage display technique identifies the interaction of severe acute respiratory syndrome coronavirus open reading frame 6 protein with nuclear pore complex interacting protein NPIPB3 in modulating Type I interferon antagonism. Journal of microbiology, immunology and infection. 2017 Jun 1;50(3):277-85.
34.Taylor JK, Coleman CM, Postel S, Sisk JM, Bernbaum JG, Venkataraman T, Sundberg EJ, Frieman MB. Severe acute respiratory syndrome coronavirus ORF7a inhibits bone marrow stromal antigen 2 virion tethering through a novel mechanism of glycosylation interference. Journal of virology. 2015 Dec 1;89(23):11820-33.
35.Pfefferle S, Krähling V, Ditt V, Grywna K, Mühlberger E, Drosten C. Reverse genetic characterization of the natural genomic deletion in SARS-Coronavirus strain Frankfurt-1 open reading frame 7b reveals an attenuating function of the 7b protein in-vitro and in-vivo. Virology journal. 2009 Dec;6(1):1-7.
36.Muth D, Corman VM, Roth H, Binger T, Dijkman R, Gottula LT, Gloza-Rausch F, Balboni A, Battilani M, Rihtarič D, Toplak I. Attenuation of replication by a 29 nucleotide deletion in SARS-coronavirus acquired during the early stages of human-to-human transmission. Scientific reports. 2018 Oct 11;8(1):1-1.
37.Sung SC, Chao CY, Jeng KS, Yang JY, Lai MM. The 8ab protein of SARS-CoV is a luminal ER membrane-associated protein and induces the activation of ATF6. Virology. 2009 May 10;387(2):402-13.
38.Mu J, Xu J, Zhang L, Shu T, Wu D, Huang M, Ren Y, Li X, Geng Q, Xu Y, Qiu Y. SARS-CoV-2-encoded nucleocapsid protein acts as a viral suppressor of RNA interference in cells. Science China Life Sciences. 2020 Sep;63(9):1-4.
39.Kang S, Yang M, Hong Z, Zhang L, Huang Z, Chen X, He S, Zhou Z, Zhou Z, Chen Q, Yan Y. Crystal structure of SARS-CoV-2 nucleocapsid protein RNA binding domain reveals potential unique drug targeting sites. Acta Pharmaceutica Sinica B. 2020 Jul 1;10(7):1228-38.
40.Zinzula L, Basquin J, Bohn S, Beck F, Klumpe S, Pfeifer G, Nagy I, Bracher A, Hartl FU, Baumeister W. High-resolution structure and biophysical characterization of the nucleocapsid phosphoprotein dimerization domain from the Covid-19 severe acute respiratory syndrome coronavirus 2. Biochemical and biophysical research communications. 2021 Jan 29; 538:54-62. s
41.Shi CS, Qi HY, Boularan C, Huang NN, Abu-Asab M, Shelhamer JH, Kehrl JH. SARS-coronavirus open reading frame-9b suppresses innate immunity by targeting mitochondria and the MAVS/TRAF3/TRAF6 signalosome. The Journal of Immunology. 2014 Sep 15;193(6):3080-9.

42.Gordon DE, Jang GM, Bouhaddou M, Xu J, Obernier K, White KM, O'Meara MJ, Rezelj VV, Guo JZ, Swaney DL, Tummino TA. A SARS-CoV-2 protein interaction map reveals targets for drug repurposing. Nature. 2020 Jul;583(7816):459-68.

43.Gao Y, Yan L, Huang Y, Liu F, Zhao Y, Cao L, Wang T, Sun Q, Ming Z, Zhang L, Ge J. Structure of the RNA-dependent RNA polymerase from COVID-19 virus. Science. 2020 May 15;368(6492):779-82.

44.Su HX, Yao S, Zhao WF, Li MJ, Liu J, Shang WJ, Xie H, Ke CQ, Hu HC, Gao MN, Yu KQ. Anti-SARS-CoV-2 activities in vitro of Shuanghuanglian preparations and bioactive ingredients. Acta Pharmacologica Sinica. 2020 Sep;41(9):1167-77.

45.Sarah Lam a, Andrew Lombardi a, Aviv Ouanounou b. COVID-19: A review of the proposed pharmacological treatmentsEuropean Journal of Pharmacology 886 (2020) 173451.

46.Balaji Gowrivel Vijayakumar, Deepthi Ramesh, Annu Joji, Jayadharini Jayachandra prakasan, Tharanikkarasu Kannan. In silico pharmacokinetic and molecular docking studies of natural flavonoids and synthetic indole chalcones against essential proteins of SARS-CoV-2 European Journal of Pharmacology Volume 886, 5 November 2020, 173448.

47.Rujuta R. Deshpande, Arpita Pandey Tiwari b, Narendra Nyayanit, Manisha Modak.In silico molecular docking analysis for repurposing therapeutics against multiple proteins from SARS-CoV-2European Journal of PharmacologyVolume 886, 5 November 2020, 173430.

48.Avinash Marwal, Mukesh Meena and R.K. Gaur. Molecular Docking Studies of Coronavirus Proteins with Medicinal Plant-Based Phytochemicals. Defence Life Science Journal, Vol. 6, No. 1, January 2021.

49.Savariar Vincent, Selvaraj Arokiyaraj, Muthupandian Saravanan and Manoj Dhanraj.Molecular Docking Studies on the Anti-viral Effects of Compounds from Kabasura Kudineer on SARS-CoV-2 3CLpro. Front. Mol. Biosci., 23 December 2020.

50.Anamika Basu1, Anasua Sarkar & Ujjwal Maulik.Molecular docking studyof potential phytochemicalsand their effects on the complexof SARS-CoV2 spike proteinand human ACE2.Scientific Reports (2020) 10:17699.

51.Sourav Das, Sharat Sarmah, Sona Lyndem and Atanu Singha Roy. An investigation into the identification of potential inhibitors of SARS-CoV-2main protease using molecular docking study. Journal of Biomolecular Structure and Dynamics 10.1080/07391102.2020.1763201.

52.Zuhal GERCEK, Deniz CEYHAN, Erol ERCAG. Synthesis and molecular docking study of novel COVID-19 inhibitors.Turkish Journal of Chemistry(2021) 45: 704-718.